J Mater Sci: Mater Med (2008) 19:1601–1608
DOI 10.1007/s10856-008-3377-6

Upregulation of matrix and adhesion molecules induced by controlled topography

K. D. Andrews · J. A. Hunt

Received: 8 September 2007 / Accepted: 4 January 2008 / Published online: 24 January 2008

Abstract Electrostatic spinning is receiving increasing attention in the field of tissue engineering, due to its ability to produce 3-dimensional, multidirectional, microfibrous scaffolds. These structures are capable of supporting a wide range of cell growth; however, there is little knowledge relating material substrates with specific cellular interactions and responses. The aim of this research was to investigate if electrostatically spun scaffolds, with controlled topographical features, would affect the adhesion mechanisms of contacting cells. A range of electrostatically spun Tecoflex® SG-80A polyurethane scaffolds was characterized in terms of inter-fibre separation, fibre diameter, surface roughness, void fraction and fibre orientation. Human embryonic lung fibroblasts and human vein endothelial cells were cultured on these scaffolds for 7, 14, 28 days, and analysed for their expression of extracellular matrix and adhesion molecules using image analysis and laser scanning confocal microscopy. There were significant differences in adhesion mechanisms between scaffolds, cell types and culture periods. Fibroblast-scaffolds were stimulated and oriented to a greater degree, and at earlier cultures, by the controlled topographical features than the endothelial cells. These conclusions confirm that cellular behaviour can be influenced by the induced scaffold topography at both molecular and cellular levels, with implications for optimum application specific tissue engineering constructs.

K. D. Andrews (✉) · J. A. Hunt
UKCTE, UKBioTEC, Division of Clinical Engineering, University of Liverpool, Duncan Building, Daulby Street, Liverpool L69 3GA, UK
e-mail: k.d.andrews@liv.ac.uk

1 Introduction

It is the ultimate goal of researchers to produce optimum application specific scaffolds for tissue engineering processes. In order to achieve this, increased knowledge into the production of these scaffolds, and their influence upon the cellular behaviour is required. It is well reported in the literature that cells respond to the underlying material substrate topography and chemistry, with variables such as morphology, coverage, cytoskeletal involvement and orientation affected. The cell behaviour has been determined as predictable, to some extent, and can occur on various cellular and molecular levels [1–4]. A wide range of extracellular matrix substrate topographies have been investigated (natural and artificial), including grooves, ridges and islands [1, 2, 5, 6]. However, porous and 3-dimensional structures have not received as much attention, including those of a fibrous nature. The naturally occurring fibrous structure of extracellular matrix produces the perfect example of optimised cell interactions, with desired phenotype expression, cell adhesion, proliferation and cytoskeletal involvement produced [3, 7–11].

The fabrication process of electrostatic spinning is capable of producing multidirectional, fibrous scaffolds with a range of structures and properties [12–17]. The production of these constructs can be achieved in a controllable, predictable manner, with a wide array of defined variables. These structures are known to support cell growth producing different cell behaviours across the range of scaffolds, and have also been determined to significantly affect both early and late stage cellular interactions [7, 18–23]. Hence, the aim of this research was to investigate if a series of electrostatically spun scaffolds, with controlled topographical features, would affect the adhesion mechanisms of contacting cells.

2 Materials and methods

2.1 Production of scaffolds

A solution of 12.5 w/v% Tecoflex® polyurethane (SG-80A, Thermedics, Woburn, USA) was mixed using polymer beads dehydrated overnight and a 1:1.68 ratio of the solvents dimethylacetamide (DMAC): 2-butanone (methyl ethyl ketone) (MEK) (Aldrich, Gillingham, UK). A range of scaffold structures was then electrostatically spun, through the systematic alteration of the spinning parameters. Parameters which were varied and controlled included: flow rate (flow of solution from nozzles); spray height (the relative vertical distance of the nozzles from the mandrel); spray distance (the horizontal distance of the nozzles from the mandrel); traverse speed (the constant linear speed of the traverse); mandrel speed (the constant rotational speed of the mandrel); grid voltage and mandrel voltage. Scaffolds were dried for 12–24 h post-production to enable their removal from the mandrels. The structures were then washed thoroughly with distilled water and dried for a further 24–48 h at 25°C.

2.2 Scaffold characterisation

Characterisation was performed with respect to: inter-fibre separation (ifs); fibre diameter (f.dia); surface roughness (SR); void fraction (VF); fibre orientation (f.orn). These structural parameters were defined as: the distance between adjacent fibres at the widest separation (ifs); the distance across a fibre edge-to-edge (f.dia); the roughness of the surface of the individual scaffold fibres (SR); the percentage of the scaffold surface area not occupied with fibrous polymeric material (VF); the angle at which fibre midlines were oriented (f.orn), with respect to the axial scaffold axis, and was measured from the span of a fibre between its junction sites (Fig. 1).

Inter-fibre separation, fibre diameter and fibre orientation were characterized using a field emission scanning electron microscope (SEM) and its incorporated digital annotation software (Leo 1550) (Leo Electron Microscopy Ltd, Cambridge, UK). Images were taken with a working distance of 8mm and an acceleration gun voltage of 5 kV, using the secondary electron detector. Measurements were taken of the structures at 1110× magnification, using the digital measuring tools, from the top layer of fibres as indicated by their overlapping on the images.

Surface roughness was measured using atomic force microscopy (AFM) (Nanoscope IIIa Scanning Probe Microscope Controller, Digital Instruments, Santa Barbara, CA, USA). Measurements were taken on an individual fibre basis, operating in contact mode, with scan sizes set to 15 μm, line scanned at a rate of 1 Hz, and a z range of 4.69 μm.

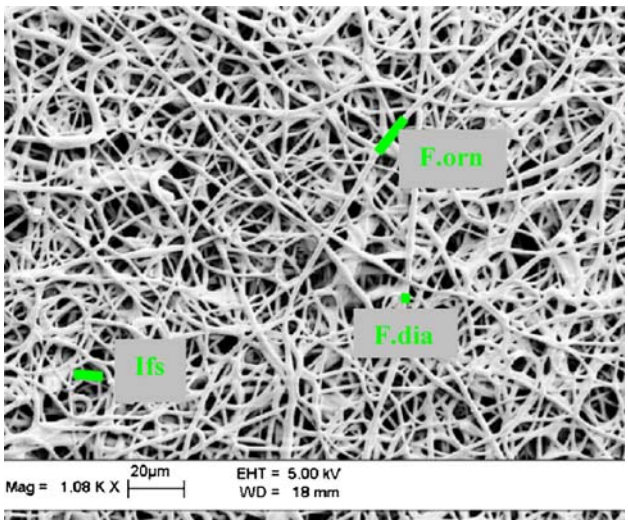

Fig. 1 SEM image showing the characterization of inter-fibre separation (ifs), fibre diameter (f.dia) and fibre orientation (f.orn)

Void fraction was quantified using the SEM images, combined with the use of the KS400 Version 3.0 imaging software package (Zeiss, Welwyn Garden City, UK); macro programs analysing the stored microscope images calculated the void areas of the scaffold.

Ifs measurements were repeated 20 times, f.dia 14 times, SR 5 times and f.orn 20 times per sample. Four repeats were performed for each scaffold examined. Means and standard error were calculated for all measurements.

2.3 Cell culture

Human embryonic lung fibroblasts (HELFs) (ECACC, Salisbury, UK) and primary derived human umbilical vein endothelial cells (HUVECs) were cultured. HELFs used 199 medium containing modified Earle's salts (Gibco™, Invitrogen Corporation, Paisley, UK), 1.25GM/L $NaHCO_3$, L-Glutamine, L-amino acids, 1% streptomycin and penicillin, and 5% bovine fetal calf serum (FCS) (Cambrex, Nottingham, UK); HUVECs were grown in 40% DMEM (Dulbecco's Modified Eagles Medium), 40% 199 (containing modified Earle's salts) (Gibco™, Invitrogen Corporation, Paisley, UK), 20% bovine fetal calf serum (FCS) (Cambrex, Nottingham, UK), 1% non-essential amino acids (NEAA), 1% sodium pyruvate, 1% streptomycin and penicillin.

Tissue culture flasks were precoated with 0.1% gelatin. HELFs were subcultured once 75–90% confluent, HUVECs once 60–80% confluent with contacting adjacent cells. Both cells required media changes every 3 days.

HELFs were seeded using cells from the 8 to 12 passages (inclusive), HUVECs from the fourth passage.

2.4 Cell-seeding of scaffolds

Scaffolds were sterilised using UV-Ozone (UV-Ozone sterilisation unit supplied by the Applied Physics Department, University of Chalmers, Sweden) (20 s per sample surface at 3 cm distance from source). The external surfaces of the scaffolds were then seeded with either HELFs or HUVECs in suspension at a seeding density of 5×10^4 cells per ml. Samples were then cultured for 7, 14 and 28 days, with media changes every 3 days. Four repeats of each culture condition were performed.

2.5 Immunohistochemistry of cell-scaffolds

Twelve sections of each cell-seeded scaffold were rinsed in Dulbeccos PBS, fixed in 4% formaldehyde 2% sucrose solution (VWR, Poole, UK) for 10 minutes at 37°C, 5% CO_2, humidified, then rinsed again with PBS. Samples were then stained with sterile filtered 0.4% methylene blue for 12 min (VWR, Poole, UK). Sample sections were incubated with rabbit serum for 30 min at room temperature, then with a 1:200 dilution of mouse anti-human primary antibodies in PBS containing 1% bovine serum albumin (BSA) at room temperature for 1 h. The primary antibodies used were: collagen I, elastin, fibronectin, CD54, CD106, CD51/61, CD49c; for HELF-scaffolds—CD49d, CD11b, CD11c; for HUVEC-scaffolds—CD31, CD62E/P, vWF. An IgG1 isotype control and PBS negative control were used throughout all staining procedures. Two PBS buffer rinses followed. Secondary antibody solution of rabbit anti-mouse immunoglobulins (biotinylated) (E0464) (Dako A/S, Denmark) (25 μl in 5ml PBS) was added for 30 min at room temperature; again followed by PBS rinses. Samples were then incubated with Vectastain ABC-AP kit (AK-500) (Vector Laboratories Inc., Burlingame, CA, USA) for 30 min. This was followed by a PBS wash. Incubation in Alkaline Phosphatase substrate (Kit 1, SK-5100) (Vector Laboratories Inc., Burlingame, CA, USA) followed (Trizma® Base (Tris[hydroxymethyl]aminomethane) (Tris) (Sigma, Gillingham, UK) solution of 1.2 g Tris in 100 ml distilled water (pH range 8.2–8.5) combined with kit reagents). Samples were incubated with this solution for 30 min in the dark, followed by a final wash step in distilled water prior to mounting in a fluorescence stabilising mountant containing DAPI nuclear stain (Vectashield® with DAPI) (Vector Laboratories Inc., Burlingame, CA, USA). Samples were kept in the dark, at 4°C, until analysis.

2.6 Analysis of cell behaviour on cell-seeded scaffolds

Cell behaviour was analysed at each culture period using reflective light microscopy, image analysis, and laser scanning confocal microscopy. Positive/negative expression of extracellular matrix and adhesion molecules was determined by reflective light microscopy and laser scanning confocal microscopy (methylene blue and DAPI nuclear stains confirmed the correct location of positive staining); quantified results were obtained through the image analysis of the images (focusing on the methylene blue staining). The mean and standard errors were calculated for all quantifiable data.

2.7 Image analysis

Image analysis of images acquired using a reflective light microscope was performed using an imaging software package (KS400, Version 3, Zeiss, Welwyn Garden City, UK): objective magnification of 20× across 20 random fields of view, with 4 repeat samples for each tested scaffold and condition, was used. Parameters investigated through the programmed macros were: cell coverage (defined as the percentage of scaffold surface covered with cells); cell number (number of cells present on the scaffold surface); cell spreading (the index of the degree of spreading of the cells, calculated by dividing the cell coverage by the cell number); cell orientation (the angle at which cells were oriented relative to the axial axis of the scaffold).

2.8 Laser scanning confocal microscopy

A laser scanning confocal microscope (LSM 510) (Zeiss, Welwyn Garden City, UK) was used to visualise the expression of the extracellular matrix and adhesion molecules and the cell nuclei. The DAPI nuclear stain was visualised at $\lambda = 364$ nm and a HeNe, $\lambda = 543$ nm laser visualised the primary antibody staining. Samples were examined at 20× magnification.

2.9 Statistics

The means and standard deviations were calculated for all quantitative data. Statistical analysis was performed by ANOVA to test the hypothesis that there were no differences in material/topographical parameters for the scaffolds; ANOVA was also used to determine the significance of variations in the cellular behaviour. This was calculated and compared between individual scaffold structures, culture time periods and cell types.

3 Results

Significant differences were found between the scaffolds produced: inter-fibre separation, fibre diameter and surface roughness (the structural components forming the physical dimensions of the scaffolds) (Fig. 2) and void fraction and fibre orientation (the components forming the 3-dimensional nature of the scaffold) (Fig. 3) were all significantly different between scaffolds ($P < 0.001$). FTIR revealed no chemical differences between the surfaces (data not shown).

Immunohistochemistry varied between scaffold, cell type and culture periods (Tables 1 and 2, Figs. 4, 5).

When examining the effect across the scaffolds, the immunohistochemistry correlated to the topographical properties (Tables 1 and 2, Figs. 4 and 5). When considering low topography scaffolds (i.e. those with few topographical features, or features not varying to any significant degree) HELFs greatly upregulated extracellular matrix molecules but few early culture adhesion molecules; HELF-scaffolds with greater topographical features showed little upregulation of extracellular matrix molecules, these being slow to "recover", and high amounts of adhesion molecules. There was also a difference seen for the HUVEC-seeded scaffolds: with little topography, HUVECs upregulated small amounts of early culture extracellular matrix and mixed amounts of adhesion molecules; with increased topography, high upregulation of extracellular matrix was observed, with a mix of adhesion molecules (Tables 1 and 2, Fig. 4).

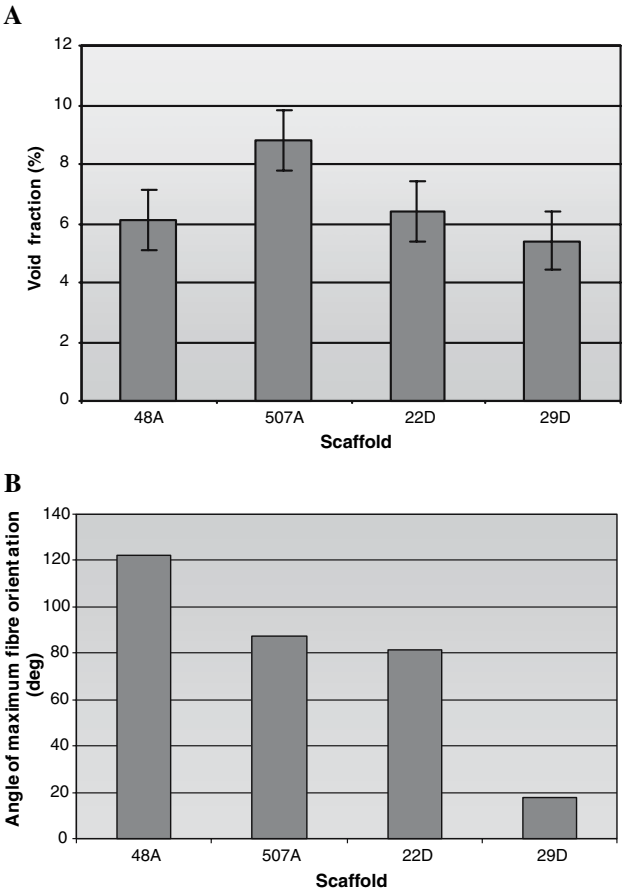

Fig. 3 Graphs showing a range of different structures produced through electrostatic spinning: (**A**) void fraction; (**B**) fibre orientation (data shown as mean ± standard error)

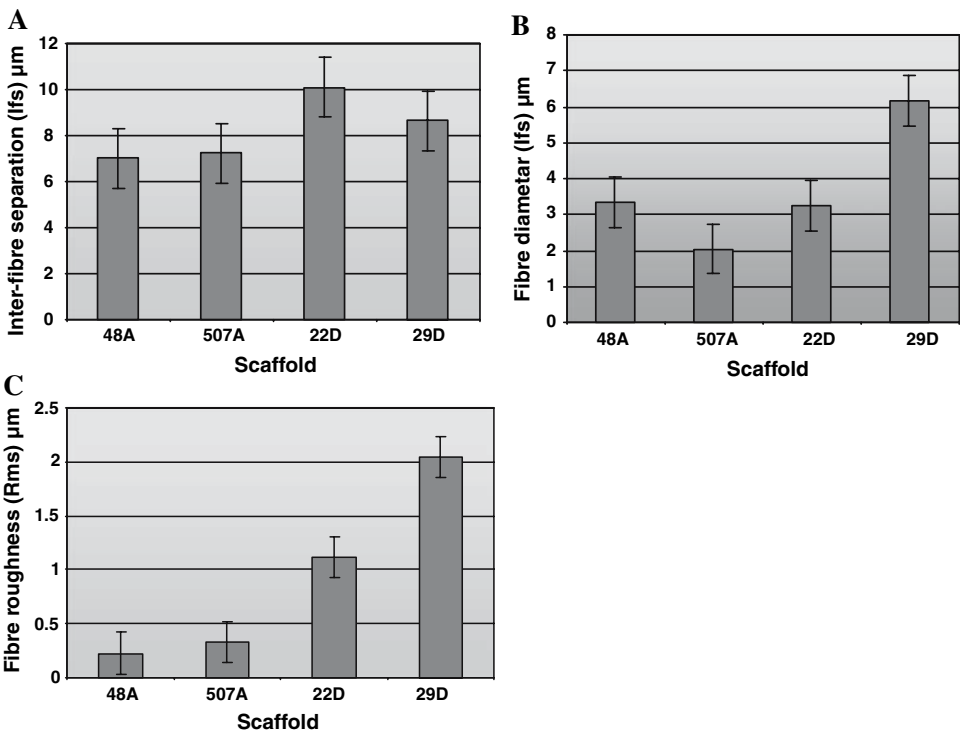

Fig. 2 Graphs showing a range of different structural dimensions produced through electrostatic spinning: (**A**) inter-fibre separation; (**B**) fibre diameter; (**C**) fibre roughness (data shown as mean ± standard error)

Table 1 Positive/negative expression of matrix and adhesion molecules for HELF-seeded scaffolds

Scaffold	Col. I	Elastin	Fibronectin	CD54	CD106	CD51/61	CD49c	CD49d	CD11b	CD11c
A. 7 days culture										
48A	+	+	+	+	−	−	−	−	−	−
507A	+	+	+	−	+	+	+	+	+	+
22D	−	−	−	+	+	+	+	+	+	+
29D	+	+	+	+	−	+	+	−	+	+
B. 14 days culture										
48A	+	+	+	+	−	−	+	+	+	+
507A	+	+	+	+	−	−	+	+	+	+
22D	+	−	+	+	−	+	+	+	+	+
29D	+	−	+	+	+	+	+	+	+	+
C. 28 days culture										
48A	+	+	+	+	−	−	+	+	+	+
507A	+	+	+	+	−	−	+	+	+	+
22D	+	−	+	+	−	+	+	+	+	+
29D	+	−	+	+	+	+	+	+	+	+

Table 2 Positive/negative expression of matrix and adhesion molecules for HUVEC-seeded scaffolds

Scaffold	Col. I	Elastin	Fibronectin	CD54	CD106	CD51/61	CD49c	CD31	CD62E/P	vWF
A. 7 days culture										
48A	−	−	+	+	+	+	−	+	−	+
507A	+	−	+	+	−	+	+	+	+	+
22D	+	+	+	+	−	+	+	−	+	+
29D	−	+	+	+	+	−	+	+	−	+
B. 14 days culture										
48A	+	+	+	+	−	+	−	+	+	−
507A	+	+	+	+	−	+	+	+	+	+
22D	+	−	+	+	−	+	−	+	+	+
29D	+	+	+	+	−	+	+	+	+	+
C. 28 days culture										
48A	+	+	+	−	+	+	+	+	−	+
507A	+	+	+	+	+	+	+	+	+	+
22D	+	+	+	+	+	+	+	+	+	+
29D	+	+	+	−	+	+	+	+	+	+

When increasing the culture period, HELF-seeded scaffolds increased their amount of both extracellular matrix and adhesion molecule expression; HUVEC-scaffolds increased their extracellular matrix but the amount of expression of adhesion molecule varied (data not specifically shown).

When examining the differences across both the scaffolds and the culture periods, the variation in expression (amount and molecule expressed) was observed between the cell types (Tables 1 and 2, and Fig. 5). HELF-scaffolds generally displayed more upregulation, mainly seen in the early culture periods.

Cell coverage, number, spreading and orientation also showed significant differences between scaffolds, cell types and culture periods ($P < 0.001$) (Fig. 6). HELF-seeded scaffolds produced greater cell coverage and numbers; HUVEC-scaffolds demonstrated comparable or greater cell spreading. HELFs increased in cell coverage, number and spreading with increasing culture period; HUVECs increased in coverage and spreading, but decreased in number.

Greater cellular orientation was seen with the HELF-scaffolds, the HUVECs exhibited a more spread morphology (Tables 1 and 2, Figs. 4 and 5).

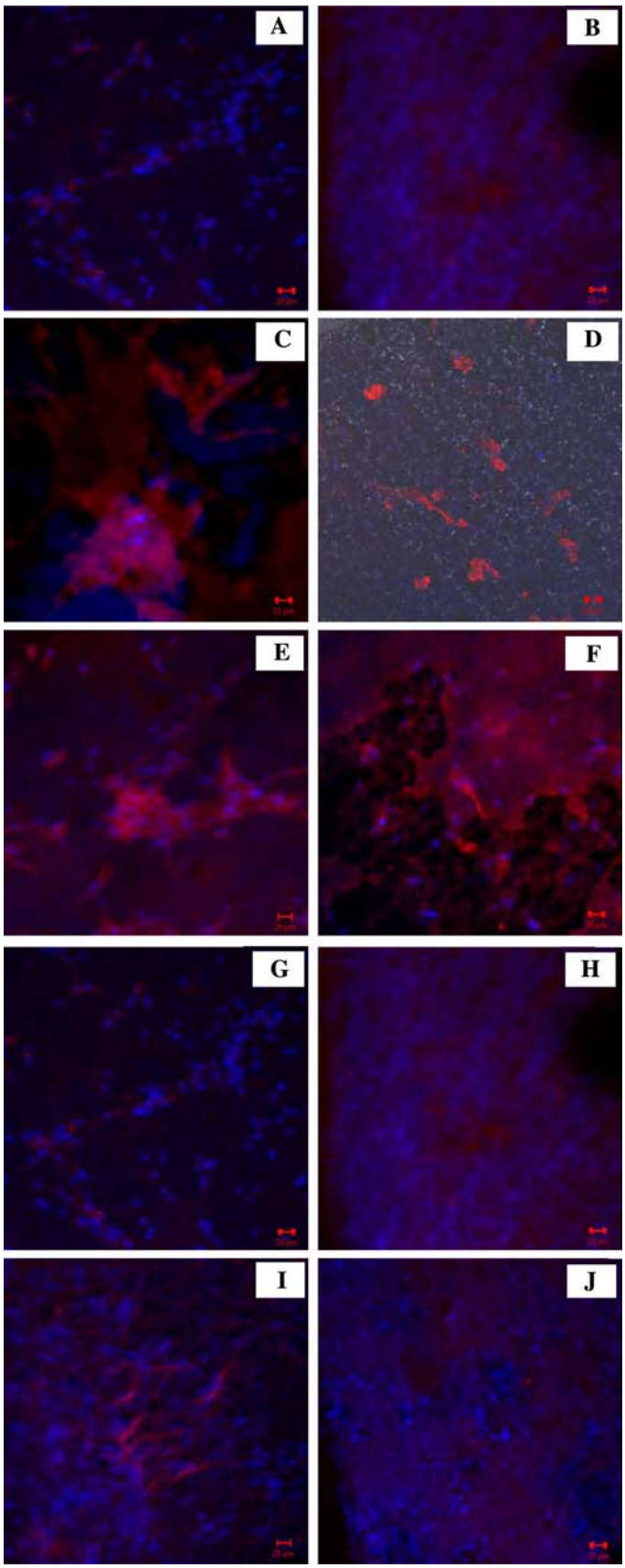

Fig. 4 Confocal images showing HELFs, 28 day culture (20× mag., red = immunostain, blue = nuclei): (**A**) scaffold 507A, collagen I; (**B**) scaffold 29D, collagen I; (**C**) 507A, fibronectin; (**D**) 29D, fibronectin; (**E**) 507A, CD51/61; (**F**) 29D, CD51/61; (**G**) 507A, CD11b; (**H**) 29D, CD11b; (**I**) 507A, CD11c; (**J**) 29D, CD11c

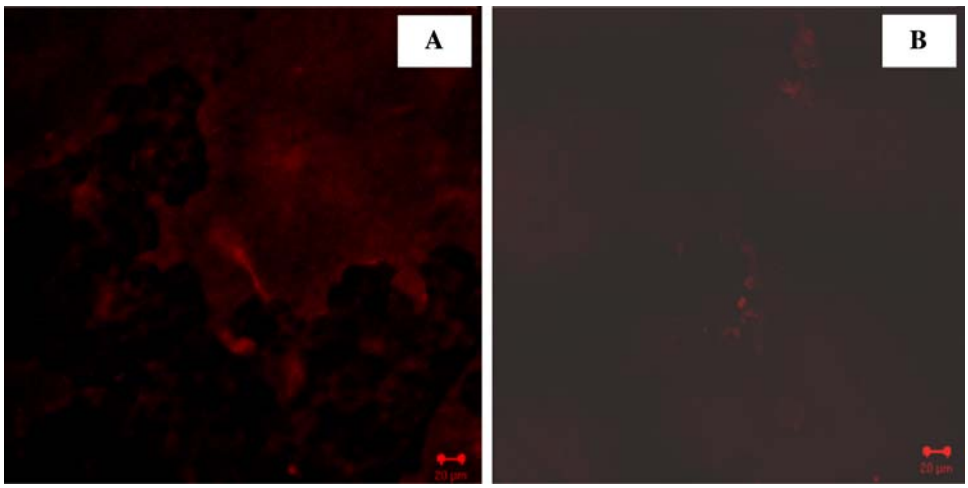

Fig. 5 Confocal images showing 28 day culture, scaffold 29D, CD51/61 (20× mag.): (**A**) HELFs; (**B**) HUVECs

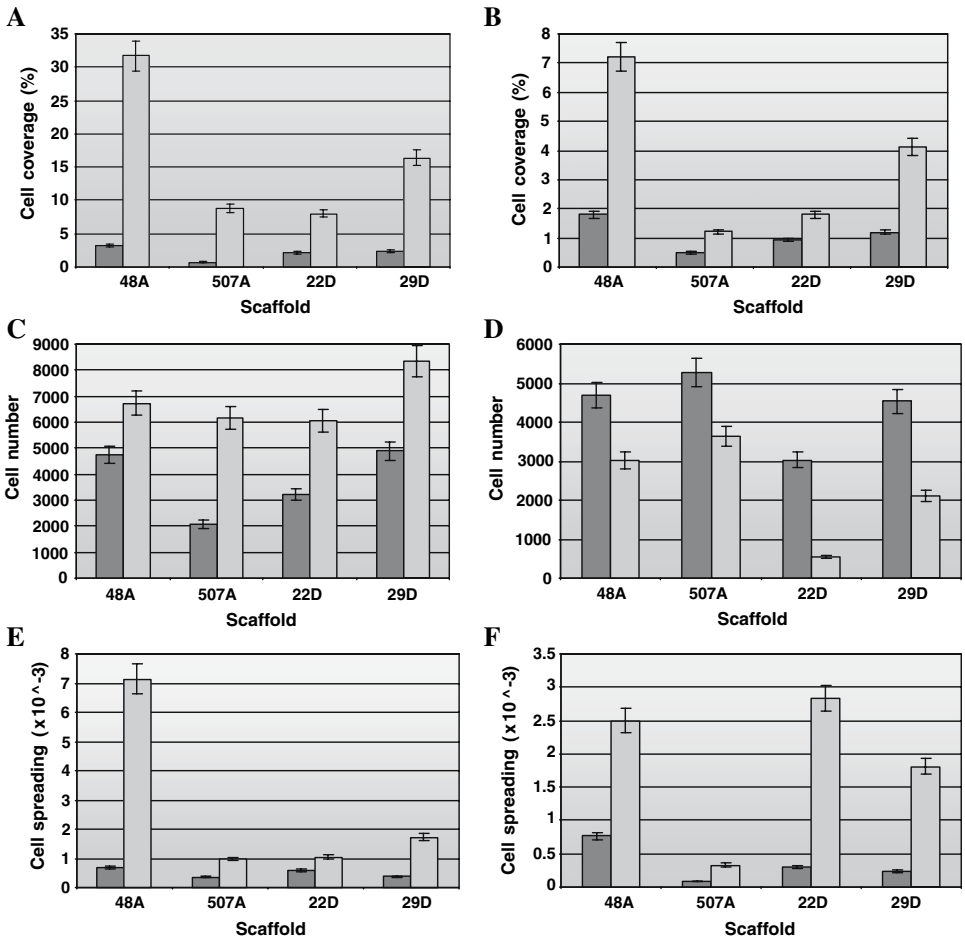

Fig. 6 Graphs showing quantitative cell data across scaffolds for HELF (dark bars) and HUVEC (light bars) seeded scaffolds for: (**A**) cell coverage at 7 days; (**B**) cell coverage at 28 days; (**C**) cell number at 7 days; (**D**) cell number at 28 days; (**E**) cell spreading at 7 days; (**F**) cell spreading at 28 days (data shown as mean ± standard error)

4 Discussion

Significantly different cellular interaction was demonstrated between the scaffolds, cell types and culture periods. These variations were detected and correlated between the quantitative cell behaviour (coverage, numbers and spreading) and the immunohistochemistry. Hence, the cells were determined to have their adhesion mechanisms significantly affected and altered, due to the fabricated differences in the topographical features (and not the chemistry, as indicated by the FTIR results).

It is well reported in literature that cells respond in a predictable manner to the underlying substrate and its topography, with adhesion, activation and proliferation all

potentially influenced [1–4]. However, studies to date have concentrated on a variety of 2-dimensional features, such as grooves and islands [1, 2, 5, 6]. Due to the recent and increasing interest in the fibrous and more 3-dimensional structures, these cellular interactions are worthy of investigation; it is likely that the sequence of cell behaviour events will be the same as seen with the 2-D structures, but with distinct mechanisms due to the increased complexity of the scaffolds [1–4, 10].

This sequence of cell-scaffolds interactions is initiated through the deposition and adsorption of extracellular matrix proteins onto the scaffold surfaces. Cell signalling pathways become activated, subsequently affecting cell adhesion, activation, proliferation and phenotype through integrin adhesion receptors and the grouping of focal contacts [8, 9, 24, 25]. These reactions can differ between cell types, with separate optimum ranges of topographical features determined [1, 2]. Generally, the more complex the topography, the greater the degree of cytoskeletal involvement and the time required for this to fully occur. This can result in a "lag" and/or a reduction in the cytoskeletal involvement, causing (if only temporarily) a reduction in the resultant cell coverage.

The variations in adhesion mechanisms determined related to cell coverage, number and spreading, with links between the extracellular matrix molecules, cell–substrate and cell–cell adhesion molecules. In general, the greater the upregulation of matrix and cell–substrate adhesion molecules, the greater the presence of cells across the scaffold surfaces (for both cell types). Fluctuation was observed for the HUVEC-scaffolds, which could be explained through the contact inhibition phenomenon naturally occurring in HUVECs. Due to their natural tendency to avoid becoming over-confluent, the adhesion molecules (cell–cell, cell–substrate and matrix) continually fluctuated to achieve a balance in cell coverage. This does not occur in the case of HELFs, hence the upregulation of molecule expression with increasing culture.

These cellular interactions also related directly to the underlying scaffold substrate. Cell mechanism trends, particularly relating to the topography were established: HELFs were found to be stimulated more than HUVECs by the topographical features, with the HUVECs initially establishing the desired levels of cell–cell contact (regardless of topography) before responding to the substrate (and so enhancing the observed "lag" period). This was also established through the greater orientation of the HELFs, as opposed to the more spread morphology of the HUVECs. The HELFs were found to be highly stimulated by increased topography, with distinct responses seen between the different levels.

5 Conclusions

Electrostatically spun scaffolds with controlled topographical features stimulated a range of cell adhesion mechanisms, varying significantly between scaffolds, cell type and culture period. Relationships with the scaffold topographical features were established: HELFs were more greatly stimulated than HUVECs, particularly at early culture periods, and showed greater specific coverage and orientation of cells.

Acknowledgements The authors acknowledge the financial support of the BBSRC, EPSRC and MRC.

References

1. A. Curtis, C. Wilkinson, Biomaterials **18**, 1573 (1997)
2. A. Curtis, C. Wilkinson, J. Biomater. Sci. Polym. Edn. **9**, 1313 (1998)
3. J. Adams, Cell. Mol. Life Sci. **58**, 371 (2001)
4. R. Flemming, C. Murphy, G. Adams, S. Goodman, P. Nealey, Biomaterials **20**, 573 (1999)
5. A. Curtis, B. Casey, J. Gallagher, D. Pasqui, M. Wood, C. Wilkinson, Biophys. Chem. **94**, 275 (2001)
6. A. Curtis, C. Wilkinson, Biochem. Soc. Symp. **65**, 15 (1999)
7. A.S. Badami, M.R. Kreke, M.S. Thompson, J.S. Riffle, A.S. Goldstein, Biomaterials **27**, 596 (2006)
8. L. Chou, J. Firth, V. Uitto, D. Brunette, J. Cell Sci. **108**, 1563 (1995)
9. E. den Braber, J. de Ruijter, L. Ginsel, A. von Recum, J. Jansen, J. Biomed. Mater. Res. **40**, 291 (1998)
10. S. Goodman, P. Sims, R. Albrecht, Biomaterials **17**, 2087 (1996)
11. P. Ma, R. Zhang, J. Biomed. Mater. Res. **46**, 60 (1999)
12. K. Andrews, J. Hunt, R. Black, Polym. Int. **57**, 203 (2008)
13. J. Doshi, D. Reneker, J. Electrostat. **35**, 151 (1995)
14. H. Jin, S. Fridrikh, G. Rutledge, D. Kaplan, Biomacromolecules **3**, 1233 (2002)
15. E. Kenawy, J. Layman, J. Watkins, G. Bowlin, J. Matthews, D. Simpson, G. Wnek, Biomaterials **24**, 907 (2003)
16. S. Koombhongse, W. Liu, D. Reneker, J. Polym. Sci. **39**, 2598 (2001)
17. J. Matthews, G. Wnek, D. Simpson, G. Bowlin, Biomacromolecules **3**, 232 (2002)
18. K. Andrews, J. Hunt, R. Black, Biomaterials **28**, 1014 (2007)
19. K. Andrews, P. Feugier, R. Black, J. Hunt, J. Surg. Res. (2007). doi:10.1016/j.jss.2007.08.030
20. H.-J. Jin, J. Chen, V. Karageorgiou, G. Altman, D. Kaplan, Biomaterials **25**, 1039 (2004)
21. B. Min, G. Lee, S. Kim, Y. Nam, T. Lee, W. Park, Biomaterials **25**, 1289 (2004)
22. X. Mo, C. Xu, M. Kotaki, S. Ramakrishna, Biomaterials **25**, 1883 (2004)
23. M. Shin, H. Yoshimoto, J. Vacanti, Tissue Eng. **10**, 33 (2004)
24. M. Dalby, S. Childs, M. Riehle, H. Johnstone, S. Affrossman, A. Curtis, Biomaterials **24**, 927 (2003)
25. M. Dalby, M. Riehle, S. Yarwood, C. Wilkinson, A. Curtis, Exp. Cell Res. **284**, 274 (2003)